SPECIAL

Thanasis Zisis

Anti-plane loading of microstructured materials in the context of couple stress theory of elasticity: half-planes and layers

Abstract The problem of calculating the displacements and stresses in a layered system often arises in engineering analysis and design, ranging from the field of mechanical engineering, to the field of materials science and soil mechanics. The present work focuses on the anti-plane response of half-planes and layers of finite thickness bonded on rigid substrates, under a point load, in the context of couple stress elasticity. The theory of couple stress elasticity is used to model the material microstructure and incorporate the size effects into the macroscopic response. This problem in plane strain configuration is referred to as Burmister's problem. The purpose is to derive the pertinent Green's functions that can be effectively used for the formulation of anti-plane contact problems in the context of couple stress elasticity. Full-field solutions regarding the out-of-plane displacements, the strains and the equivalent stress are presented, and of special importance is the behavior of the new solutions near to the point of application of the force where pathological singularities and discontinuities exist in the classical solutions.

Keywords Anti-plane problems · Couple stress elasticity · Micromechanics · Bonded layer

1 Introduction

The present work focuses on the anti-plane response of microstructured half-planes and microstructured layers of finite thickness bonded on rigid substrates, under a surface point force. Anti-plane shear deformations describe simple classes of deformations that solids can undergo. In anti-plane shear of a cylindrical body for example, the displacement is parallel to the generators of the cylinder and is independent of the axial coordinate. Thus anti-plane shear, with just a single axial displacement field, may be viewed as complementary to the more complicated but more familiar plane strain deformation, with its two in-plane displacements. For this reason, the anti-plane problems play an important role as benchmark problems allowing for various aspects of solutions in solid mechanics to be examined in the context of a simple setting [3,16,17,26,32].

The problem of calculating the stresses and displacements in a layered elastic system is one which often arises in engineering analysis and design in areas as mechanical engineering, material science as well as soil mechanics—Burmister [5]. The simplest case of layered system is that of an elastic layer bonded on a rigid base. A further important aspect of such problems is the introduction of the material microstructural characteristics of the layer within the analysis and the incorporation of possible size effects.

Classical continuum theories cannot explain size effects exhibited by many materials at the micron and nanometer scales due to the lack of any material length scale parameter and for this reason, higher-order elasticity theories have been proposed in order to interpret the microstructure-dependent size effects upon the

T. Zisis (✉)
Mechanics Division, School of Applied Mathematics and Physical Science, National Technical University of Athens,
15773 Athens, Greece
E-mail: zisis@mail.ntua.gr

elastic properties. Such theories include the Cosserat theory [6], the couple stress theories [8,19,21] and the strain gradient elasticity theories [22,29,30].

One effective generalized continuum theory is that of *couple stress* elasticity, also known as *Cosserat theory* with constrained rotations [21,29]. In this theory, the strain energy density and the resulting constitutive relations involve, besides the usual infinitesimal strains, certain strain gradients known as the rotation gradients. The generalized stress-strain relations for the isotropic case include, in addition to the conventional pair of elastic constants, two new elastic constants, one of which is expressible in terms of a material parameter ℓ that has dimension of length. The presence of this length parameter, in turn, implies that the modified theory encompasses the analytical possibility of size effects, which are absent in the classical theory. Furthermore, the conventional stress tensor is no longer symmetric and the antisymmetric part of the stress tensor, as well as the isotropic part of the couple stress tensor remain indeterminate.

As $\ell \to 0$, both of the new elastic constants vanish and the classical elastic theory is recovered. The theory is different from the Cosserat (referenced also as micropolar) theory that takes material particles with six independent degrees of freedom (three displacement components and three rotation components, the latter involving rotation of a micro-medium w.r.t its surrounding medium). Sometimes, the name restricted Cosserat theory appears in the literature for the couple stress theory.

We note that couple stress elasticity had already in the 1960s some successful application on stress concentration problems concerning holes and inclusions (see e.g., [2,23,28,31]). In recent years, problems of dislocations, plasticity, fracture and wave propagation have been re-analyzed within the framework of couple stress theory. This is due to the inability of the classical theory to predict experimental observed size effects and also due to the increased demands for manufacturing devices at very small scales. Recent applications include work by, among others, Lubarda and Markenskoff [20], Barbet and Vardoulakis [1], Georgiadis and Velgaki [10], Grentzelou and Georgiadis [15], and Radi [24], Zisis et al. [33], Zisis et al. [34], Gourgiotis and Zisis [11], Gourgiotis et al. [12]. An interesting exposition of orthotropic couple stress theory in anti-plane configuration was presented by Gourgiotis and Bigoni, ([13,14], *Part I and Part II*).

2 Anti-plane formulation

For a body that occupies a domain in the (x, y)-plane under anti-pane conditions, the displacement field takes the general form:

$$u_x \equiv 0, \quad u_y \equiv 0, \quad u_z \equiv w(x, y) \neq 0. \tag{1}$$

The non-vanishing components of strain, rotation and curvature [dimensions of $(\text{length})^{-1}$], in the framework of geometrically linear theory, are given as:

$$\varepsilon_{xz} = \varepsilon_{zx} = \frac{1}{2}\partial_x w, \quad \varepsilon_{yz} = \varepsilon_{yz} = \frac{1}{2}\partial_y w, \tag{2}$$

$$\omega_x = \omega_{yz} = \frac{1}{2}\partial_y w, \quad \omega_y = \omega_{xz} = -\frac{1}{2}\partial_x w, \tag{3}$$

$$\kappa_{xx} = -\kappa_{yy} = \frac{1}{2}\partial_x \partial_y w, \quad \kappa_{xy} = -\frac{1}{2}\partial_x^2 w, \quad \kappa_{yx} = \frac{1}{2}\partial_y^2 w \tag{4}$$

whereas the constitutive equations furnish:

$$\tau_{xz} = 2\mu\varepsilon_{xz} = \mu\partial_x w, \quad \tau_{yz} = 2\mu\varepsilon_{yz} = \mu\partial_y w, \tag{5}$$

$$m_{xx} = 4(\eta + \eta')\kappa_{xx} = 2(\eta + \eta')\partial_x \partial_y w, \tag{6}$$

$$m_{yy} = 4(\eta + \eta')\kappa_{yy} = -2(\eta + \eta')\partial_x \partial_y w = -m_{xx}, \tag{7}$$

$$m_{xy} = 4\eta\kappa_{xy} + 4\eta'\kappa_{yx} = -2\eta\partial_x^2 w + 2\eta'\partial_y^2 w, \tag{8}$$

$$m_{yx} = 4\eta\kappa_{yx} + 4\eta'\kappa_{xy} = 2\eta\partial_y^2 w - 2\eta'\partial_x^2 w, \tag{9}$$

In (5)–(9), τ_{ij} are the usual symmetric stresses while m_{ij} are deviatoric part of the couple stresses expressed in dimensions of $(\text{force})(\text{length})^{-1}$. Note that the scalar $\mu_{\kappa\kappa}$ of the couple stress tensor does not appear in the final equation of equilibrium, nor in the reduced boundary conditions and the constitutive equations. Consequently, it is left indeterminate within the couple stress theory. The modulus μ has the same meaning as the Lamé constants of classical elasticity theory and is expressed in dimensions of $(\text{force})(\text{length})^{-2}$, whereas

the moduli (η, η') account for couple stress effects and are expressed in dimensions of (force). The following restrictions for the material constants should prevail on the basis of a positive definite strain energy density [21]

$$3\lambda + 2\mu > 0, \quad \mu > 0, \quad \eta > 0, \quad -1 < \frac{\eta'}{\eta} < 1. \tag{10}$$

Accordingly, the non-vanishing components of the antisymmetric part of the force-stress tensor are written as—for vanishing body moments ([13], *Part I*):

$$\alpha_{zx} = -\alpha_{xz} = \frac{1}{2}\left(\partial_x m_{xy} + \partial_y m_{yy}\right) = \eta\partial_x\left(\nabla^2 w\right), \tag{11}$$

$$\alpha_{zy} = -\alpha_{yz} = -\frac{1}{2}\left(\partial_x m_{xx} + \partial_y m_{yx}\right) = \eta\partial_y\left(\nabla^2 w\right). \tag{12}$$

Finally by taking into account (11), (12), and noting that the total stress tensor σ_{ij} (which is asymmetric) can be decomposed into a symmetric and antisymmetric part as:

$$\sigma_{ij} = \tau_{ij} + \alpha_{ij} \tag{13}$$

Equation (13) suggests that the total stress can be decomposed into a symmetric and an antisymmetric part. Note further that the antisymmetric part is not derived from constitutive equations but can be found from the conservation of angular momentum (balance of moments).

Furthermore, the total stress can be written in terms of out-of-plane displacement as:

$$\sigma_{xz} = \mu\partial_x\left(w - \ell^2\nabla^2 w\right), \tag{14}$$

$$\sigma_{zx} = \mu\partial_x\left(w + \ell^2\nabla^2 w\right), \tag{15}$$

$$\sigma_{yz} = \mu\partial_y\left(w - \ell^2\nabla^2 w\right), \tag{16}$$

$$\sigma_{zy} = \mu\partial_y\left(w + \ell^2\nabla^2 w\right), \tag{17}$$

where $\ell = (\eta/\mu)^{1/2}$.

In view of the above and by enforcing equilibrium, a single *Partial Differential Equation* (PDE) of the fourth order for the displacement component is obtained:

$$\nabla^2 w - \ell^2\nabla^4 w = 0. \tag{18}$$

Regarding traction boundary conditions, at any point on a smooth boundary or section, the following force-traction and tangential couple-traction should be specified [19,21]

$$P_z^{(n)} = \sigma_{yz} + \frac{1}{2}\partial_x m_{yy} \tag{19}$$

$$R_x^{(n)} = m_{yx}. \tag{20}$$

As expected, in the limit of $\ell \to 0$ Eq. (18) reduces to the equation of classical linear isotropic elasticity for anti-plane problems is recovered. Indeed the fact that Eq. (18) has an increased order with respect to the limit case of classical elasticity and the length and the fact that the coefficient ℓ multiplies the higher-order term reveal the singular-perturbation character of the couple stress theory and the emergence of associated boundary-layer effects.

Both parameters, the microstructural length ℓ and the cross-sensitivity constant $\beta = \eta'/\eta$, depend upon the microstructure and can be connected to the material characteristic lengths in bending and torsion as [24]:

$$\ell_b = \ell/\sqrt{2}, \quad \ell_t = \ell\sqrt{1 + \beta}. \tag{21}$$

Typical values of the parameters ℓ_b and ℓ_t for materials with microstructure are referenced in Radi [24]. For example, a syntactic foam that consists of hollow glass micro-bubbles embedded in an epoxy matrix has $\ell_b = 0.032$ and $\ell_t = 0.065$ mm ($\ell = 0.045$ mm and $\beta = 1$). A high-density rigid polyurethane closed cell foam has $\ell_b = 0.0327$ and $\ell_t = 0.62$ mm ($\ell = 0.462$ mm and $\beta = 0.797$). The limit value of $\beta = -1$ corresponds to a vanishing characteristic length in torsion, which is typical of polycrystalline metals. Furthermore, for $\beta = -0.5$, $\ell_b = \ell_t$ and for $\beta = 0$, $\ell = \sqrt{2}\ell_b = \ell_t$.
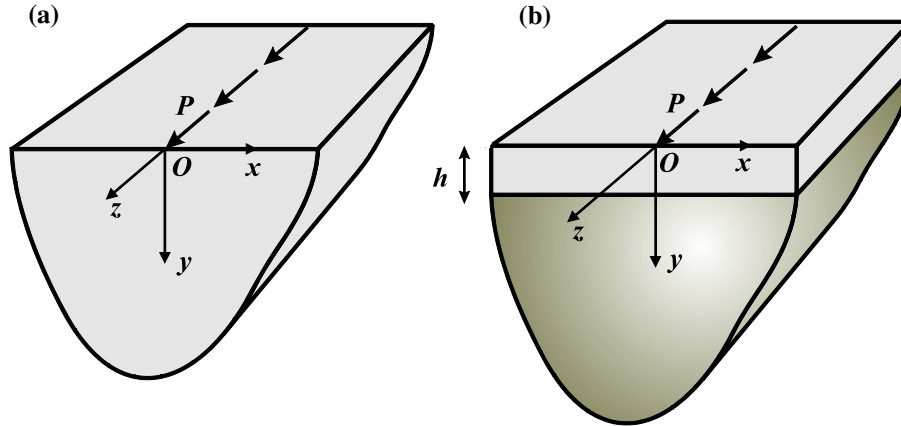
Fig. 1 Schematic representation of the problem. A concentrated force acts on the surface of **a** a microstructured half-plane, **b** a microstructured layer of thickness h. The layer adheres on a rigid substrate. In both cases, the material characteristics are described through the shear modulus μ, the Poisson's ratio ν and the moduli (η, η') that account for the couple stress effects

At this point, we should note that an analogue can be formulated from the area of structural mechanics which is the Kirchhoff plate under biaxial tensile prestress where the shear forces stem from bending due to in-plate initial tensile stress. The tensile equal-biaxial in plane prestress serves to build a Helmholtz type of equilibrium as shown in (18). A simple inspection between the related equations of the Kirchhoff plate with prestress and the anti-plane couple stress formulation suggests a direct analogy. In other words, one can obtain either the out-of-plane displacement field of the couple stress anti-plane case or the vertical displacement of the Kirchhoff plate with prestress by knowing the solution of either problem. Further details regarding this analogue and its incorporation into commercial finite element codes can be seen on a separate publication by Gavardinas et al. [9].

3 Loading by a concentrated anti-plane force

We now consider the displacement field produced in an elastic half-plane and a layer of finite thickness bonded on a rigid substrate under the action of a concentrated anti-plane force as shown in Fig. 1 (a and b, respectively). The body is governed by the equations of couple stress elasticity, and a Cartesian coordinate system $Oxyz$ is attached to the geometry.

3.1 Boundary conditions

3.1.1 Half-plane under the action of a concentrated anti-plane force

For the anti-plane force case, the following traction boundary conditions at the surface of the half-plane ($y = 0$) apply (for details the reader is referred to [19,21]:

$$m_{yx}(x, 0) = 0, \text{ at } -\infty < x < \infty \tag{22}$$

$$t_{yz}(x, 0) = \sigma_{yz}(x, 0) + \frac{1}{2}\partial_x m_{yy}(x, 0) = P\delta(x), \text{ at } -\infty < x < \infty \tag{23}$$

where P is the magnitude of the force along the z direction, as shown in Fig. 1, and $\delta(x)$ is the Dirac function.

3.1.2 Layer bonded on a rigid substrate under the action of a concentrated anti-plane force

Regarding the tractions at the surface of the layer ($y = 0$) we write:

$$m_{yx}(x, 0) = 0, \text{ at } -\infty < x < \infty \tag{24}$$

$$t_{yz}(x,0) = \sigma_{yz}(x,0) + \frac{1}{2}\partial_x m_{yy}(x,0) = P\delta(x), \text{ at } -\infty < x < \infty \tag{25}$$

while the out-of-plane displacements and their gradient at $y = h$ (bottom of the bonded layer) are:

$$w(x,h) = 0 \quad \text{at } -\infty < x < \infty, \tag{26}$$

$$\frac{\partial w(x,y)}{\partial y} = 0 \quad \text{at } -\infty < x < \infty. \tag{27}$$

In the context of classical elasticity, the corresponding boundary conditions for the case of the layer read:

$$t_{yz}(x,0) = \sigma_{yz}(x,0) = P\delta(x), \text{ at } -\infty < x < \infty \tag{28}$$
$$w(x,h) = 0 \text{ at } -\infty < x < \infty. \tag{29}$$

4 Fourier transform analysis

The two traction boundary value problems described above are attacked by using the Fourier transform. We proceed by introducing the Fourier transform in x, viz.,

$$\hat{f}(\xi) = \int_{-\infty}^{\infty} f(x)e^{i\xi x}\mathrm{d}x, \tag{30}$$

for the exponential Fourier transform of a function f that is defined and is suitably regular on $(-\infty, \infty)$, ξ being the real-valued transform parameter. According to the appropriate inversion theorem, (30) implies,

$$f(x) = \frac{1}{2\pi}\int_{-\infty}^{\infty} \hat{f}(\xi)e^{-i\xi x}\mathrm{d}\xi, \tag{31}$$

where $i \equiv (-1)^{1/2}$.

Next we apply the Fourier transform to the couple stresses m_{yx} and stresses t_{yz} to obtain:

$$\hat{m}_{yx} = 2\eta\left(\frac{\mathrm{d}^2\hat{w}}{\mathrm{d}y^2} + \xi^2\beta\hat{w}\right), \tag{32}$$

and

$$\hat{t}_{yz} = \mu\left(\left(1 + (2+\beta)\,\xi^2\ell^2\right)\frac{\mathrm{d}\hat{w}}{\mathrm{d}y} - \ell^2\frac{\mathrm{d}^3\hat{w}}{\mathrm{d}y^3}\right). \tag{33}$$

Accordingly, general PDE (18) in the transformed domain reads:

$$\ell^2\frac{\mathrm{d}^4\hat{w}}{\mathrm{d}y^4} - \left(1 + 2\ell^2\xi^2\right)\frac{\mathrm{d}^2\hat{w}}{\mathrm{d}y^2} + \xi^2\left(1 + \ell^2\xi^2\right)\hat{w} = 0, \tag{34}$$

5 Solution of the problem

5.1 Half-plane under the action of a concentrated anti-plane force

Solving Eq. (34) for bounded displacements as $y \to +\infty$, we get a general solution for the homogeneous half-plane of the following general form:

$$\hat{w} = \left[C_1(\xi)\,e^{-|\xi|y} + C_2(\xi)\,e^{-\delta y}\right], \tag{35}$$

where $\delta = \sqrt{\frac{1}{\ell^2} + \xi^2}$.

The following transformed boundary conditions apply at the surface of the half-plane:

$$\hat{m}_{yx}(\xi, 0) = 0 \text{ and } \hat{t}_{yz}(\xi, 0) = P, \tag{36}$$

and accordingly $C_1(\xi)$ and $C_2(\xi)$ can be expressed as:

$$C_1(\xi) = \frac{-P\left(1 + \ell^2\xi^2(1+\beta)\right)}{\mu\left(|\xi| + 2\ell^2|\xi|^3(1+\beta) + \ell^4\xi^4\left(|\xi| - \sqrt{\frac{1}{\ell^2} + \xi^2}\right)(1+\beta)^2\right)},$$

$$C_2(\xi) = \frac{\ell^2 P\xi^2(1+\beta)}{\mu\left(|\xi| + 2\ell^2|\xi|^3(1+\beta) + \ell^4\xi^4\left(|\xi| - \sqrt{\frac{1}{\ell^2} + \xi^2}\right)(1+\beta)^2\right)}. \tag{37}$$

Then, the transformed out-of-plane displacement for the half-plane as given by Eq. (35) takes the form:

$$\hat{w}(\xi, y) = \frac{e^{-\left(|\xi| + \sqrt{\frac{1}{\ell^2} + \xi^2}\right)y}\left(e^{|\xi|y}\ell^2 P\xi^2(1+\beta) - e^{\sqrt{\frac{1}{\ell^2} + \xi^2}y}P\left(1 + \ell^2\xi^2(1+\beta)\right)\right)}{\mu\left(|\xi| + 2\ell^2|\xi|^3(1+\beta) + \ell^4\xi^4\left(|\xi| - \sqrt{\frac{1}{\ell^2} + \xi^2}\right)(1+\beta)^2\right)}, \tag{38}$$

and at the surface $y = 0$ is found to be (note that it is an even function of ξ):

$$\hat{w}(\xi, 0) = \frac{-P}{\mu\left(|\xi| + 2\ell^2|\xi|^3(1+\beta) + \ell^4\xi^4\left(|\xi| - \sqrt{\frac{1}{\ell^2} + \xi^2}\right)(1+\beta)^2\right)}. \tag{39}$$

The transformed out-of-plane displacement $\hat{w}(\xi, 0)$ may be written as:

$$\hat{w}(\xi, 0) = -\frac{P}{\mu|\xi|} + \frac{\ell^2 P}{\mu\left(1 + \ell^2\xi^2\right)^{1/2}} + \frac{P|\xi|\left(1 + \ell^2 q\xi^2\left(2 + \ell^2 q\left(\delta^2 + \xi^2\right)\right) - 2\ell^2 q\delta\left(1 + \ell^2 q\xi^2\right)|\xi|\right)}{\mu\delta\left(|\xi| + 2\ell^2|\xi|^3 q + \ell^4\xi^4\left(|\xi| - \delta\right)q^2\right)}, \tag{40}$$

where $q = 1 + \beta$.

Examination of (40) suggests that it is an even function of ξ, and by employing theorems of the Abel-Tauber type [25] the asymptotic behavior of the out-of-plane displacement w at $y = 0$, as $x \to 0$, is bounded in contrast to classical elasticity, while as $x \to \infty$ the logarithmic behavior observed in classical elasticity is retained also in couple stress elasticity.

For reference purposes and completeness, we write the corresponding solution for the out-of-plane displacement in the context of classical elasticity. We begin by expressing the single constant of the solution of the transformed PDE that corresponds to the classical elasticity and can be derived upon transformation of (18) upon setting $\ell = 0$. In this case, the solution of the corresponding transformed PDE has the general form:

$$\hat{w}_{\text{class}}(\xi, y) = -\frac{P}{\mu\sqrt{\xi^2}}e^{-|\xi|y}. \tag{41}$$

5.1.1 Layer adhered on a rigid substrate under the action of a concentrated anti-plane force

We proceed by presenting the corresponding solution for the case of a layer bonded on a rigid substrate. For the case of the concentrated force at its surface, by solving Eq. (34), we obtain the following general solution:

$$\hat{w} = A_1(\xi)e^{-|\xi|y} + A_2(\xi)e^{-\delta y} + A_3(\xi)e^{|\xi|y} + A_4(\xi)e^{\delta y}, \tag{42}$$

where $\delta = \sqrt{\frac{1}{\ell^2} + \xi^2}$.

Assuming a layer of finite thickness h, transformed boundary conditions (24)–(27) suggest:

$$A_1(\xi) = \frac{-e^{-h\delta}P\left(-2e^{h\delta}\ell^2 q\delta\xi^2 - e^{h(2\delta + |\xi|)}\left(1 + \ell^2 q\xi^2\right)\left(-\delta + |\xi|\right) + e^{h|\xi|}\left(1 + \ell^2 q\xi^2\right)\left(\delta + |\xi|\right)\right)}{4\mu|\xi|\left(\delta T_1 + 2\ell^2 q\xi^2\left(1 + \ell^2 q\xi^2\right)\left(T_1 - 1\right) - \xi\left(1 + \left(1 + \ell^2 q\xi^2\right)\left(2 + q + 2\ell^2 q\xi^2\right)\right)T_2\right)} \tag{43}$$

$$A_2(\xi) = \frac{-e^{-h\delta}P\left(-2e^{h|\xi|}|\xi|\left(1 + \ell^2 q\xi^2\right) + e^{h(\delta + 2|\xi|)}\ell^2 q\xi^2\left(-\delta + |\xi|\right) + e^{h\delta}\ell^2 q\xi^2\left(\delta + |\xi|\right)\right)}{4\mu|\xi|\left(\delta T_1 + 2\ell^2 q\xi^2\left(1 + \ell^2 q\xi^2\right)\left(T_1 - 1\right) - \xi\left(1 + \left(1 + \ell^2 q\xi^2\right)\left(2 + q + 2\ell^2 q\xi^2\right)\right)T_2\right)} \tag{44}$$

$$A_3(\xi) = \frac{e^{-h(\delta + |\xi|)}P\left(\left(\left(e^{2h\delta} + 1\right)\delta + \left(e^{2h\delta} - 1\right)|\xi|\right)\left(1 + \ell^2 q\xi^2\right) - 2e^{h(\delta + |\xi|)}\ell^2 q\delta\xi^2\right)}{4\mu|\xi|\left(\delta T_1 + 2\ell^2 q\xi^2\left(1 + \ell^2 q\xi^2\right)\left(T_1 - 1\right) - \xi\left(1 + \left(1 + \ell^2 q\xi^2\right)\left(2 + q + 2\ell^2 q\xi^2\right)\right)T_2\right)} \tag{45}$$

$$A_4(\xi) = \frac{e^{-h(\delta+|\xi|)} P \left(2e^{h(\delta+|\xi|)} |\xi| \left(1 + \ell^2 q\xi^2\right) - e^{2h|\xi|}\ell^2 q\xi^2 \left(\delta + |\xi|\right) + \ell^2 q \left(\delta\xi^2 - |\xi|^3\right)\right)}{4\mu |\xi| \left(\delta T_1 + 2\ell^2 q\xi^2 \left(1 + \ell^2 q\xi^2\right)(T_1 - 1) - \xi \left(1 + \left(1 + \ell^2 q\xi^2\right)\left(2 + q + 2\ell^2 q\xi^2\right)\right) T_2\right)} \tag{46}$$

where $T_1 = T_1(\xi, h, \beta) = \cos(h\delta)\cos(h\xi)$, $T_2 = T_2(\xi, h, \beta) = \sin(h\delta)\sin(h\xi)$ and $\delta = \sqrt{\frac{1}{\ell^2} + \xi^2}$, $q = 1 + \beta$.

The anti-plane displacement is an even function of ξ, and at the surface of the layer ($y = 0$) reads:

$$\hat{w}(\xi, 0)$$
$$= \frac{-P \left(\xi \cosh(h\xi)\sinh(h\delta) - \delta \cosh(h\delta)\sinh(h\xi)\right)}{\mu\xi \left(-\delta \left(1 + 2\ell^2 q\xi^2 \left(1 + \ell^2 q\xi^2\right)\right) T_1 + \xi \left(2\ell^2 q\delta\xi \left(1 + \ell^2 q\xi^2\right) + \left(1 + \ell^2 q\xi^2 \left(2 + q + 2\ell^2 q\xi^2\right)\right) T_2\right)\right)}. \tag{47}$$

Equation (47) suggests that the asymptotic behavior of the out-of-plane displacement w at $y = 0$, as $x \to 0$, is bounded in contrast to classical elasticity, while as $x \to \infty$ the logarithmic behavior observed in the case of the half-plane is eliminated due to the finite thickness of the layer. Furthermore, for $h \to \infty$, Eq. (39) is recovered as expected.

The corresponding classical elasticity transformed solution is now given for reference purposes. The solution of the transformed PDE has the general form $\hat{w} = A_{1\text{class}}(\xi) e^{-|\xi|y} + A_{2\text{class}}(\xi) e^{|\xi|y}$, and the constants $A_{1\text{class}}(\xi)$ and $A_{2\text{class}}(\xi)$ are evaluated by the appropriate boundary conditions for $\ell = 0$. This results to:

$$A_{1\text{class}}(\xi) = -\frac{P}{\mu |\xi|} \frac{e^{2h|\xi|}}{1 + e^{2h|\xi|}} \quad \text{and} \quad A_{2\text{class}}(\xi) = \frac{P}{\mu |\xi|} \left(1 - \frac{e^{2h|\xi|}}{1 + e^{2h|\xi|}}\right), \tag{48}$$

and the transformed out-of-plane displacement takes the following form:

$$\hat{w}_{\text{class}}(\xi, y, h) = \hat{w} = -\frac{P\text{sech}(h\xi)\sinh((h - y)\xi)}{\mu\xi}, \tag{49}$$

which at the surface of the layer ($y = 0$) reduces to:

$$\hat{w}_{\text{class}}(\xi, 0, h) = \hat{w} = -\frac{P\tanh(h\xi)}{\mu\xi}. \tag{50}$$

For $h \to \infty$, Eq. (41) is recovered.

6 Fourier transform inversion

In what follows, we calculate the displacement field and present details regarding the strains, the curvatures, the stresses and the couple stresses. The solution will determine the behavior of the out-of-plane displacement near the point of application of the concentrated force and will allow detecting the deviations from the classical theory of elasticity. The determination of the displacement stress or strain field inside the half-plane ($y \neq 0$) follows along the same general lines of the present analysis with additional numerical work; thus, further details are omitted.

6.1 Half-plane under the action of a concentrated anti-plane force

For the case of the half-plane, the anti-plane displacement w at the surface ($y = 0$) can be written in terms of three integrals:

$$w(x, 0) = I_{CE} + I_{CS-1} + I_{CS-2}, \tag{51}$$

where, according to (40):

$$I_{CE} = -\frac{P}{\pi\mu} \int_0^\infty \frac{1}{\xi} \cos(\xi x) \, d\xi, \tag{52}$$

$$I_{CS-1} = \frac{\ell^2 P}{\pi \mu} \int_0^\infty \frac{1}{\left(1 + \ell^2 \xi^2\right)^{1/2}} \cos\left(\xi x\right) d\xi, \tag{53}$$

$$I_{CS-2} = \frac{P}{\pi \mu} \int_0^\infty \frac{|\xi|\left(1 + \ell^2 q \xi^2 \left(2 + \ell^2 q \left(\delta^2 + \xi^2\right)\right)\right) - 2\ell^2 q \delta \left(1 + \ell^2 q \xi^2\right) |\xi|\right)}{\delta \left(|\xi| + 2\ell^2 |\xi|^3 q + \ell^4 \xi^4 \left(|\xi| - \delta\right) q^2\right)} \cos\left(\xi x\right) d\xi. \tag{54}$$

The first two integrals in (53) can be obtained in closed form, whereas the third integral has to be numerically evaluated. The first integral is in fact divergent but can be efficiently evaluated by using results of the theory of distributions in the *Finite Part* sense giving $I_{CE} = \frac{P}{\pi \mu} \log |x|$, while the second integral is convergent and is evaluated as $I_{CS-1} = \frac{P}{\mu} K_0 \left[\frac{|x|}{\ell}\right]$, where K_0 is the modified Bessel function of the second kind.

The anti-plane surface displacements after appropriate normalization ($x = \bar{x}\ell$ and $\xi = \bar{\xi}/\ell$) follow directly as:

$$\bar{w}\left(\bar{x}, 0\right) = \frac{w\left(\bar{x}, 0\right) \mu}{P}$$

$$= \frac{\log |\bar{x}|}{\pi} + K_0 \left[|\bar{x}|\right] + \frac{1}{\pi} \int_0^\infty \frac{\left(1 - q\bar{\xi} \left(\sqrt{1 + \bar{\xi}^2} - \bar{\xi}\right)\right)^2}{\sqrt{1 + \bar{\xi}^2} \left(1 + q\bar{\xi}^2 \left(2 - q\bar{\xi} \left(-\bar{\xi} + \sqrt{1 + \bar{\xi}^2}\right)\right)\right)} \cos\left(\bar{\xi}\bar{x}\right) d\bar{\xi} \tag{55}$$

where $q = 1 + \beta$.

The normalized strains $\{\bar{\varepsilon}_{ij}\} = \frac{\mu \ell}{P} \{\varepsilon_{xz}, \varepsilon_{yz}\}$ and the normalized curvatures $\{\bar{\kappa}_{ij}\} = \frac{\mu \ell^2}{P} \{\kappa_{xx}, \kappa_{yy}, \kappa_{yx},$ $\kappa_{xy}\}$ are calculated directly from (55). In fact it can be shown, by employing theorems of the Abel–Tauber type and examining the behavior of the transformed strains and curvatures as $\xi \to \infty$ that:

$$\begin{cases} \{\bar{\varepsilon}_{ij}\} = O\left(1\right) \\ \{\bar{\kappa}_{ij}\} = O\left(\log \bar{r}\right) \end{cases}, \quad \text{for } \bar{r} \to 0 \tag{56}$$

with $\bar{r} = \sqrt{\bar{x}^2 + \bar{y}^2}$.

Furthermore, regarding the stresses and couple stresses, Eq. (56), suggests that:

$$\begin{cases} \{\bar{\tau}_{ij}\} = O\left(1\right) \\ \{\bar{m}_{ij}\} = O\left(\log \bar{r}\right) \\ \{\bar{\sigma}_{ij}|_{i \neq j}\} = O\left(\bar{r}^{-1}\right) \end{cases}, \quad \text{for } \bar{r} \to 0 \tag{57}$$

For reference we provide the corresponding normalized classical elasticity full-field solution, which reads:

$$\bar{w}\left(\bar{x}, \bar{y}\right) = \frac{w\left(\bar{x}, \bar{y}\right) \mu}{P} = \frac{\log\left(\bar{x}^2 + \bar{y}^2\right)}{2\pi}, \tag{58}$$

$$\bar{\varepsilon}_{xz}\left(\bar{x}, \bar{y}\right) = \frac{\varepsilon_{xz}\left(\bar{x}, \bar{y}\right) \ell \mu}{P} = \frac{\bar{x}}{2\pi \left(\bar{x}^2 + \bar{y}^2\right)}, \tag{59}$$

$$\bar{\varepsilon}_{yz}\left(\bar{x}, \bar{y}\right) = \frac{\varepsilon_{yz}\left(\bar{x}, \bar{y}\right) \ell \mu}{P} = \frac{1}{2\pi} \int_0^\infty e^{-\bar{y}\bar{\xi}} \cos\left(\bar{\xi}\bar{x}\right) d\bar{\xi} = \frac{1}{2\pi} \frac{\bar{y}}{\bar{x}^2 + \bar{y}^2}, \tag{60}$$

$$\bar{\sigma}_{xz}\left(\bar{x}, \bar{y}\right) = \bar{\sigma}_{zx}\left(\bar{x}, \bar{y}\right) = \frac{\sigma_{xz}\left(\bar{x}, \bar{y}\right) \ell}{P} = \frac{\bar{x}}{\pi \left(\bar{x}^2 + \bar{y}^2\right)}, \tag{61}$$

$$\bar{\sigma}_{yz}\left(\bar{x}, \bar{y}\right) = \bar{\sigma}_{zy}\left(\bar{x}, \bar{y}\right) = \frac{\sigma_{yz}\left(\bar{x}, \bar{y}\right) \ell}{P} = \frac{\bar{y}}{\pi \left(\bar{x}^2 + \bar{y}^2\right)}, \tag{62}$$

where $\bar{y} = y/\ell$.

6.2 Layer bonded on a rigid substrate under the action of a concentrated anti-plane force

When the half-plane is replaced by a layer of finite thickness h, loaded by a concentrated force at its surface, the out-of-plane surface displacements w, after appropriate normalization ($x = \bar{x}\ell$, $\xi = \bar{\xi}/\ell$ and $h = \bar{h}\ell$) and by assuming that $\xi \geq 0$, can be written as:

$$\bar{w}(\bar{x}, 0) = \frac{w(\bar{x}, 0)\,\mu}{P} = \frac{1}{\pi} \int_0^\infty \hat{w}(\bar{\xi}, 0, h) \cos(\bar{\xi}\bar{x})\, d\bar{\xi} \tag{63}$$

where $\hat{w}(\bar{\xi}, 0, h)$ is given by Eq. (47).

The normalized strains $\{\bar{\varepsilon}_{ij}\} = \frac{\mu\ell}{P}\{\varepsilon_{xz}, \varepsilon_{yz}\}$, the normalized stresses $\{\bar{\sigma}_{ij}\} = \frac{\ell}{P}\{\sigma_{xz}, \sigma_{zx}, \sigma_{yz}, \sigma_{zy}\}$ and the normalized couple stresses $\{\bar{m}_{ij}\} = \frac{1}{P}\{m_{xx}, m_{yy}, m_{xy}, m_{yx}\}$ are calculated directly from (63).

We also provide the corresponding normalized classical elasticity solution, which reads:

$$\bar{w}(\bar{x}, \bar{y}) = \frac{w(\bar{x}, \bar{y})\,\mu}{P} = -\frac{1}{\pi} \int_0^\infty \frac{\operatorname{sech}(\bar{h}\bar{\xi}) \sinh((\bar{h} - \bar{y})\bar{\xi})}{\bar{\xi}} \cos(\bar{\xi}\bar{x})\, d\bar{\xi} \tag{64}$$

or at the surface:

$$\bar{w}(\bar{x}, 0) = \frac{w(\bar{x}, 0)\,\mu}{P} = -\frac{1}{\pi} \int_0^\infty \frac{\tanh(\bar{h}\bar{\xi})}{\bar{\xi}} \cos(\bar{\xi}\bar{x})\, d\bar{\xi}, \text{ at } y = 0 \tag{65}$$

while $\bar{w}(\bar{x}, 0)|_{h \to \infty} = \frac{w(\bar{x},0)\mu}{P} = \frac{\log(\bar{x})}{\pi}$.

We note that in the case of the layer of finite thickness, the calculated displacements are exact and should not be interpreted only qualitatively but also quantitatively. This is not true for the case of the half-plane, where $w(x, y)$ can only be defined relative to an arbitrary chosen datum [4].

Furthermore, the normalized strains $\bar{\varepsilon}_{xz}$ and $\bar{\varepsilon}_{yz}$ read, respectively:

$$\bar{\varepsilon}_{xz}(\bar{x}, 0) = \frac{\varepsilon_{xz}(\bar{x}, 0)\,\ell\mu}{P} = \frac{1}{2\pi} \int_0^\infty \operatorname{sech}(\bar{h}\bar{\xi}) \sinh(s(\bar{h} - \bar{y})) \sin(\bar{x}\bar{\xi})\, d\bar{\xi}, \tag{66}$$

$$\bar{\varepsilon}_{yz}(\bar{x}, \bar{y}) = \frac{\varepsilon_{yz}(\bar{x}, \bar{y})\,\ell\mu}{P} = -\frac{1}{2\pi} \int_0^\infty \operatorname{sech}(\bar{h}\bar{\xi}) \cosh(\bar{\xi}(\bar{h} - \bar{y})) \sin(\bar{\xi}\bar{x})\, d\bar{\xi}. \tag{67}$$

Integrals (63) and (64)–(67) can be efficiently evaluated numerically.

7 Results and discussion

Representative results are shown in Figs. 2 and 3 for the case of the half-plane. The normalized out-of-plane displacement $w\mu/P$ and strains $\varepsilon_{xz}\mu\ell/P$ and $\varepsilon_{yz}\mu\ell/P$ are presented along the surface of the half-plane for different values of β (see Fig. 2). These results may be seen in conjunction to the contour plots for the out-of-plane displacements, and the strains shown in Fig. 3a–c, respectively.

For cross-sensitivity constant $\beta = -1$, the classical elasticity results are recovered. This case corresponds to a vanishing characteristic length in torsion, typical of polycrystalline metals, the classical elasticity solution is essentially recovered and contours of the out-of-plane displacements w exhibit *semi-circular* shape and present a logarithmic behavior as $\bar{r} \to 0$. The ε_{xz} strain component becomes infinite as $O(r^{-1})$ at the point of the application of the load while the ε_{yz} strain component vanishes at the surface.

In mark contrast, for increasing cross-sensitivity constant β, the out-of-plane displacements as well as the strains become bounded at the point of the application of the load while the shape of the corresponding out-of-plane displacement contours is *semi-elliptical* (Fig. 3a).

It should be noted that at $x = y = 0$, $\varepsilon_{xz}\mu\ell/P = 0$ while $\varepsilon_{yz}\mu\ell/P$ presents a gradient discontinuity. It is further concluded that outside the point of the application of the load, $\varepsilon_{xz}\mu\ell/P$ decreases for increasing β. Furthermore, at $x = y = 0$, $\varepsilon_{yz}\mu\ell/P$ decreases for increasing β. It is underlined that the couple stress effects are dominant up to $x/\ell \approx 3$ from the point of the application of the load while further away their effect deteriorates.

As a final comment, we should point out that the logarithmic behavior of the of the out-of-plane displacement prevails as $x/\ell \to \infty$. Thus, the quantitative results of the out-of-plane displacements should be received up
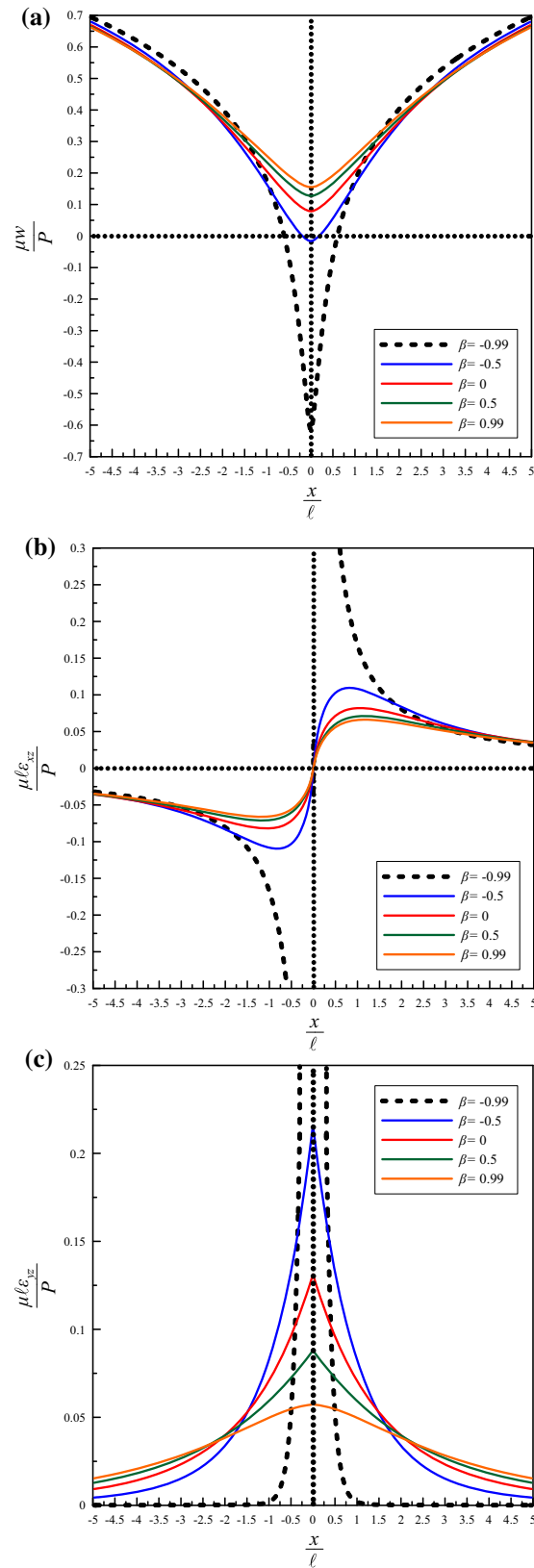
Fig. 2 Homogeneous half-plane—concentrated anti-plane force P. Normalized (**a**) anti-plane displacement w and strains (**b**) ε_{xz}, **c** ε_{yz}, along the surface of the half-plane as a function of β respectively
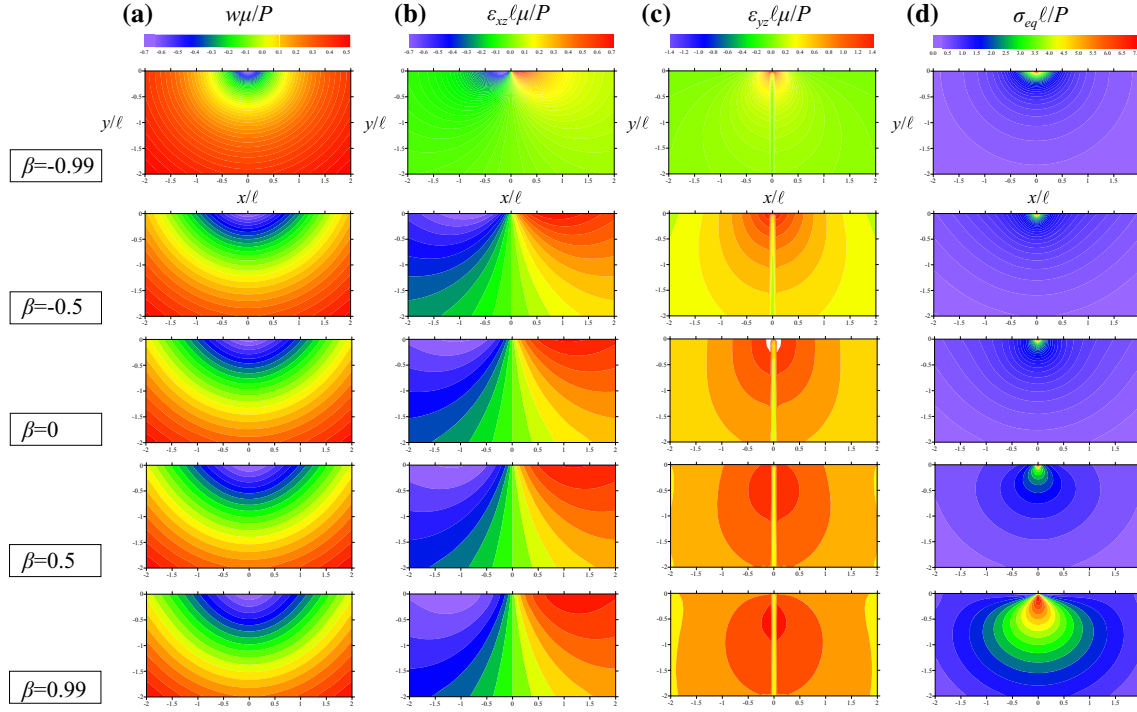
Fig. 3 Homogeneous half-plane—normalized contour fields for **a** out-of-plane displacement w, strains **b** ε_{xz}, **c** ε_{yz}, and **d** equivalents stresses σ_{eq} for selected values of β respectively

to a rigid body motion. This is also observed in classical theory of elasticity, is related to the two dimensional nature of the problem and has been discussed in [18] and Bower [4].

It is further instructive to examine the equivalent stress in order identify the severest state stress and accordingly the potential regions with respect to the point of the application of the force, that plasticity may emanate. In the case of couple stress and according to J_2-flow theory, following de Borst [7] and Shu and Fleck [27], we introduce a general form of the normalized equivalent stress as:

$$\frac{\sigma_{eq}\ell}{P} = \left(3 \left(\frac{1}{4} \left(\bar{\sigma}_{xz}^2 + \bar{\sigma}_{zx}^2 + \bar{\sigma}_{yz}^2 + \bar{\sigma}_{zy}^2 \right) + \frac{1}{4} \left(2\bar{\sigma}_{xz}\bar{\sigma}_{zx} + 2\bar{\sigma}_{yz}\bar{\sigma}_{zy} \right) + \frac{1}{2} \left(\bar{m}_{xx}^2 + \bar{m}_{xy}^2 + \bar{m}_{yy}^2 + \bar{m}_{yx}^2 \right) \right) \right)^{1/2}.$$
(68)

In an anti-plane configuration the equivalent stress as shown in Eq. (68) reduces to (69).

$$\frac{\sigma_{eq}\ell}{P} = \left(3 \left(\bar{\tau}_{xz}^2 + \bar{\tau}_{yz}^2 + \frac{1}{2} \left(\bar{m}_{xx}^2 + \bar{m}_{xy}^2 + \bar{m}_{yy}^2 + \bar{m}_{yx}^2 \right) \right) \right)^{1/2},$$
(69)

Alternatively, in classical elasticity Eq. (68) takes the following form:

$$\frac{\sigma_{eq}\ell}{P} = \left(3 \left(\bar{\tau}_{xz}^2 + \bar{\tau}_{yz}^2 \right) \right)^{1/2}.$$
(70)

Our analysis showed that in couple stress elasticity the behavior of the equivalent stress is $O\left(\log \bar{r}\right)$ as $\bar{r} \to 0$ while in classical elasticity a more severe behavior is attained, that is $O\left(\bar{r}^{-1}\right)$ as $\bar{r} \to 0$. The effect of β upon the equivalent stress is shown in Fig. 3d for the case of the half-plane and in Figs. 5 and 6 for the case of the bonded layer. We note that for $\beta = -0.99$ (essentially the classical elasticity case) the severest state of stress is observed at the point of the application of the load and at its immediate circular periphery, while at the other extreme, that is $\beta = 0.99$, the contours of the equivalent stress exhibit major qualitative differences. In this case, the stress becomes less severe immediately below the point of the application of the load—$O\left(\log \bar{r}\right)$— while both a vertical and a perpendicular expansion is observed. This is somewhat similar to the case of contact for Hertzian geometries where the severest state of stress does not lie immediately beneath the contact area. It should be noted that a severe state of stress is attained in this case for $y \approx 0.25\ell$ below the point of the
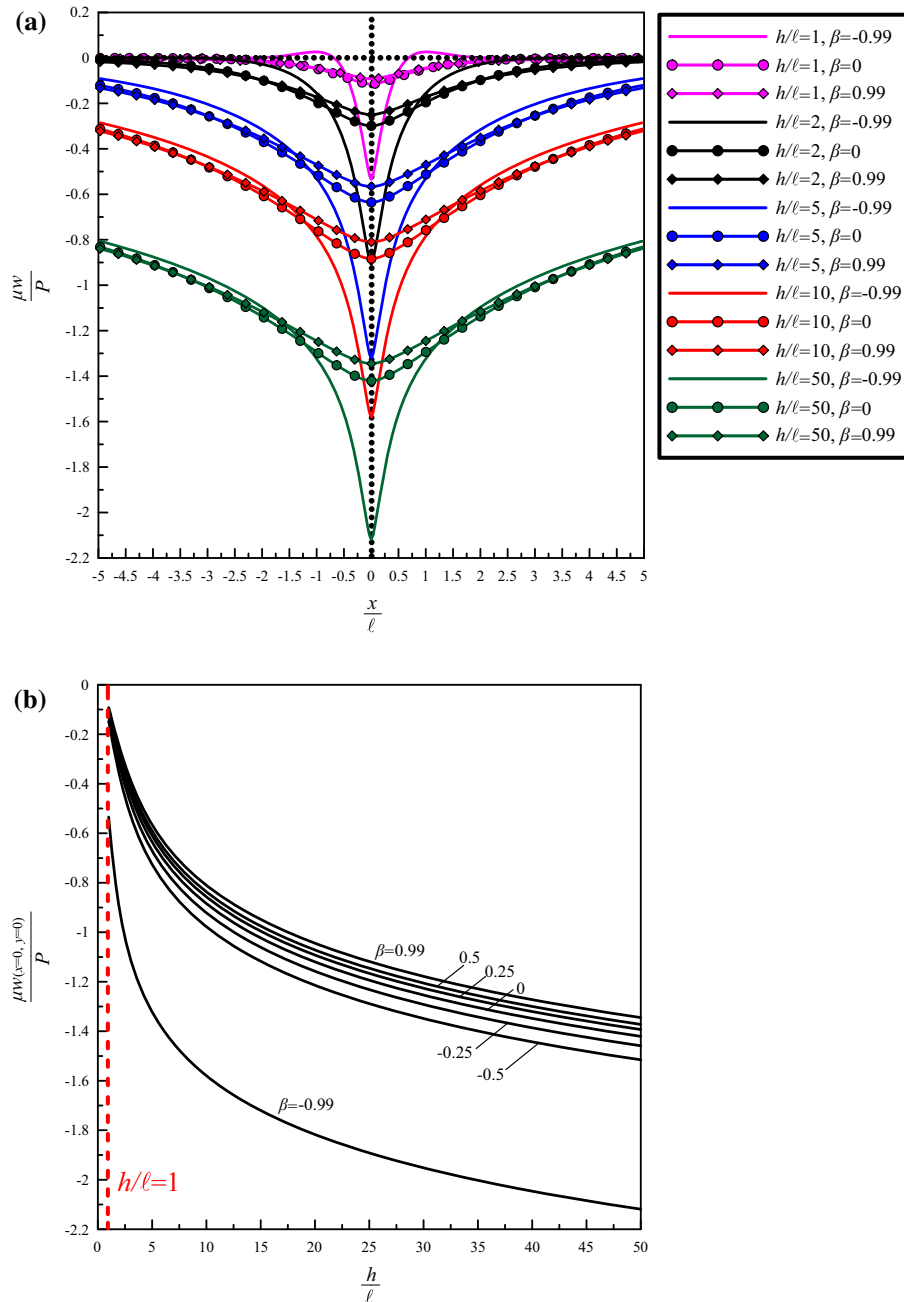
Fig. 4 Layer adhered on a rigid substrate. **a** Profile of the normalized out-of-plane displacement w at the surface of the layer for selected values of for selected values of β and h/ℓ. **b** Normalized out-of-plane displacement w at the point of the application of the load as a function of the layer thickness for selected values of β

application of the force (see Fig. 3d). When the equivalent stress reaches the material yield stress, yielding will commence—although the plastic enclave will be surrounded by elastic material—and at loads modestly above the elastic limit might be approximated in shape by one of the contours in Fig. 3d.

In the case of the layer bonded on a rigid substrate and subjected to an anti-plane force, representative results are shown in Figs. 4, 5 and 6. Regarding the displacements, the stresses and the strains, the results are quantitatively similar to the case of the half-plane with a mark contrast associated with the surface displacements, which away from the point of the application of the load vanish. As β departs from -1 the displacement at $(x, y) = (0, 0)$ becomes bounded and its maximum reduces progressively for increasing β and decreasing
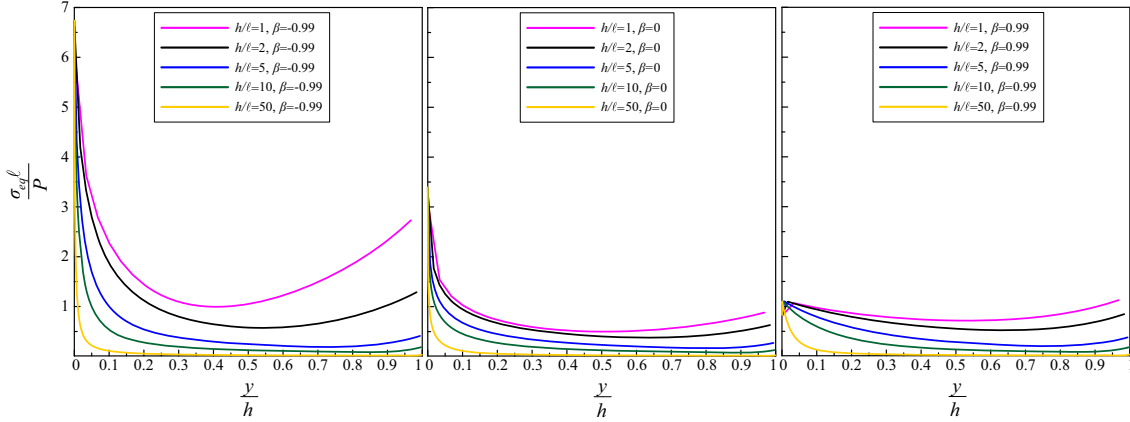
Fig. 5 Normalized equivalent stress $\sigma_{eq}\ell/P$ for layer adhered on a rigid substrate along the symmetry axis $x = 0$ for selected values of β and h/ℓ
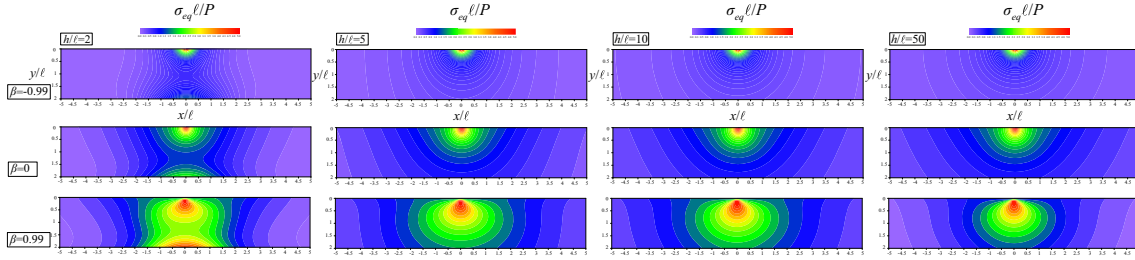

Fig. 6 Layer adhered on a rigid substrate. Normalized contours of equivalent stress $\sigma_{eq}\ell/P$ for selected values of β and h/ℓ

h/ℓ suggesting a stiffer response. Furthermore, the thinner the layer the more confined is the deformation zone (Figs. 4b). Interestingly, for $h/\ell = 1$ which should physically be considered as a limiting case, the out-of-plane displacements immediately outside the point of the application of the load change sign designating what could be described as a pile-up effect in terms of contact mechanics. In Figs. 5 and 6, we present the equivalent stress along the symmetry axis, $x = 0$, as well as contours of the normalized equivalent stress, both for selected values of β and h/ℓ. Near the point of the application of the load, the behavior of the equivalent stress is qualitatively similar to what is observed in the case of the half-plane and no further comment is in need. If we focus at the interface between the layer and the rigid substrate ($y = h$) we note that for fixed microstructural length ℓ decreasing layer thickness or for decreasing β, increased equivalent stresses are observed which would suggest the occurrence of possible plastic regions or delamination.

8 Conclusions

In the present work, we studied the anti-plane response of half-planes and layers of finite thickness that adhere on rigid substrates, under the action of a point load on the surface, in the context of couple stress elasticity in order to incorporate the material microstructural characteristics. The anti-plane problems play an important role as benchmark problems allowing for various aspects of solutions in solid mechanics to be examined in the context of a simple setting and these solutions are presented for the first time in the context of couple stress elasticity. Through the use of integral transforms, we derived the pertinent Green's functions that can be used as the "*building block*" for the formulation of more involved anti-plane contact problems.

Here, we revealed interesting deviations from the predictions of anti-plane classical linear elasto-statics through examination of the asymptotic behavior as well as the presentation of the full-field solutions of the out-of-plane displacements, the strains and the equivalent stress with respect to the microstructural characteristics and the thickness of the layer. Of special importance is the behavior of the new solutions near to the point of application of the load, where pathological singularities and discontinuities exist in the classical solutions, and at the interface referring to the layer. Furthermore, the effect of β upon the stress state was examined through the introduction of the equivalent stress for the case of couple stress elasticity.

References

1. Bardet, J.-P., Vardoulakis, I.: The asymmetry of stress in granular media. Int. J. Solids Struct. **38**(2), 353–367 (2001)
2. Bogy, D.B., Sternberg, E.: The effect of couple-stresses on singularities due to discontinuous loadings. Int. J. Solids Struct. **3**(5), 757–770 (1967)
3. Borrelli, A., Horgan, C.O., Patria, M.C.: Saint–Venant's principle for anti-plane shear deformations of linear piezoelectric materials. SIAM J. Appl. Math. **62**, 2027–2044 (2002)
4. Bower, A.F.: Applied Mechanics of Solids. CRC Press, Boca Raton (2009)
5. Burmister, D.M.: Evaluation of pavement systems of the WASHO road test by layered system methods. Highw. Res. Board Bull. **177**, 26–54 (1958)
6. Cosserat, E., Cosserat, F.: Theorie Des Corps Deformables. Herman, Paris (1909)
7. de Borst, R.: A generalisation of J2-flow theory for polar continua. Comput. Methods Appl. Mech. Eng. **103**(3), 347–362 (1993)
8. Eringen, A.C.: Nonlinear Theory of Continuous Media. McGraw-Hill, New York (1962)
9. Gavardinas, I.D., Giannakopoulos, A.E. Zisis, T.: A pre-stressed plate analogue for solving anti-plane problems in couple stress and dipolar elasticity. Int. J. Solids. Struct. (2017) (**under review**)
10. Georgiadis, H.G., Velgaki, E.G.: High-frequency Rayleigh waves in materials with micro-structure and couple-stress effects. Int. J. Solids Struct. **40**(10), 2501–2520 (2003)
11. Gourgiotis, P.A., Zisis, T.: Two-dimensional indentation of microstructured solids characterized by couple-stress elasticity. J. Strain Anal. Eng. Des. **51**(4), 318–331 (2016)
12. Gourgiotis, P.A., Zisis, T., Baxevanakis, K.P.: Analysis of the tilted flat punch in couple-stress elasticity. Int. J. Solids Struct. **85**, 34–43 (2016)
13. Gourgiotis, P.A., Bigoni, D.: Stress channelling in extreme couple-stress materials part I: strong ellipticity, wave propagation, ellipticity, and discontinuity relations. J. Mech. Phys. Solids **88**, 150–168 (2016)
14. Gourgiotis, P.A., Bigoni, D.: Stress channelling in extreme couple-stress materials part II: localized folding vs faulting of a continuum in single and cross geometries. J. Mech. Phys. Solids **88**, 169–185 (2016)
15. Grentzelou, C.G., Georgiadis, H.G.: Uniqueness for plane crack problems in dipolar gradient elasticity and in couple-stress elasticity. Int. J. Solids Struct. **42**(24), 6226–6244 (2005)
16. Horgan, C.O.: Anti-plane shear deformation in linear and nonlinear solid mechanics. SIAM Rev. **37**, 53–81 (1995)
17. Horgan, C.O., Miller, K.L.: Anti-plane shear deformation for homogeneous and inhomogenuous anisotropic linearly elastic solids. J. Appl. Mech. **61**, 23–29 (1994)
18. Johnson, K.L.: Contact Mechanics. Cambridge University Press, Cambridge (1987)
19. Koiter, W.T.: Couple-stresses in the theory of elasticity, I & II. Philos. Trans. R. Soc. Lond. B. **67**, 17–44 (1969)
20. Lubarda, V.A., Markenscoff, X.: Conservation integrals in couple stress elasticity. J. Mech. Phys. Solids **48**(3), 553–564 (2000)
21. Mindlin, R.D., Tiersten, H.F.: Effects of couple-stresses in linear elasticity. Arch. Ration. Mech. Anal. **11**, 415–448 (1962)
22. Mindlin, R.D.: Micro-structure in linear elasticity. Arch. Ration. Mech. Anal. **16**(1), 51–78 (1964)
23. Mindlin, R.D.: Influence of couple-stresses on stress concentrations. Exp. Mech. **3**(1), 1–7 (1963)
24. Radi, E.: On the effects of characteristic lengths in bending and torsion on mode III crack in couple stress elasticity. Int. J. Solids Struct. **45**(10), 3033–3058 (2008)
25. Roos, B.W.: Analytic Functions and Distributions in Physics and Engineering. Wiley, NewYork (1969)
26. Sofonea, M., Dalah, M., Ayadi, A.: Analysis of an anti-plane electro-elastic contact problem. Adv. Math. Sci. Appl. **17**, 385–400 (2007)
27. Shu, J.Y., Fleck, N.A.: The prediction of a size effect in microindentation. Int. J. Solids Struct. **35**(13), 1363–1383 (1998)
28. Takeuti, Y., Noda, N.: Thermal stresses and couple-stresses in square cylinder with a circular hole. Int. J. Eng. Sci. **11**(5), 519–530 (1973)
29. Toupin, R.A.: Elastic materials with couple-stresses. Arch. Ration. Mech. Anal. **11**(1), 385–414 (1962)
30. Toupin, R.A.: Theories of elasticity with couple-stress. Arch. Ration. Mech. Anal. **17**(2), 85–112 (1964)
31. Weitsman, Y.: Couple-stress effects on stress concentration around a cylindrical inclusion in a field of uniaxial tension. J. Appl. Mech. **32**(2), 424–428 (1965)
32. Zhou, Z.-G., Wang, B., Du, S.-Y.: Investigation of anti-plane shear behavior of two collinear permeable cracks in a piezo-electric material by using the nonlocal theory. J. Appl. Mech. **69**, 1–3 (2002)
33. Zisis, T., Gourgiotis, P.A., Baxevanakis, K.P., Georgiadis, H.G.: Some basic contact problems in couple stress elasticity. Int. J. Solids Struct. **51**(11), 2084–2095 (2014)
34. Zisis, T., Gourgiotis, P.A., Dal Corso, F.: A contact problem in couple stress thermoelasticity: the indentation by a hot flat punch. Int. J. Solids Struct. **63**, 226–239 (2015)